Interface optical phonons in spheroidal quantum dots

2002 J. Phys.: Condens. Matter 14 6469

(http://iopscience.iop.org/0953-8984/14/25/314)

INSTITUTE OF PHYSICS PUBLISHING JOURNAL OF PHYSICS: CONDENSED MATTER

J. Phys.: Condens. Matter **14** (2002) 6469–6481 PII: S0953-8984(02)33893-1

Interface optical phonons in spheroidal quantum dots

F Comas[1], C Trallero-Giner[1], N Studart[2] and G E Marques[2]

[1] Departamento de Física Teórica, Universidad de la Habana, Vedado 10400, Havana, Cuba
[2] Departamento de Física, Universidade Federal de São Carlos, 13565-905 São Carlos, São Paulo, Brazil

Received 18 February 2002, in final form 1 May 2002
Published 14 June 2002
Online at stacks.iop.org/JPhysCM/14/6469

Abstract

Interface optical phonons are studied in the case of a quantum dot (QD) with prolate and oblate spheroidal geometries within the dielectric continuum approach. We considered CdSe or CdS QDs imbedded in a host material which is modelled as an infinite medium. The surface optical phonon modes, the corresponding frequencies, and the electron–phonon interaction Hamiltonian are reported. Comparison is made with previous works which only considered strictly spherical dots. We conclude that deviations from the perfect spherical shape could be responsible for observable physical effects in Raman spectra.

1. Introduction

The theoretical investigation of polar optical vibrations in small-size crystals was initiated a long time ago [1] by applying a continuum dielectric model valid in the long-wavelength limit. In this approach, both bulk-like oscillations and surface modes are included in the study of the vibrations of finite samples. The quantum version of such oscillatory modes are the well-known longitudinal optical (LO) and transverse optical (TO) bulk-like phonons and the corresponding surface optical (SO) phonons. Weakly polar semiconductor compounds, in the form of slabs and spheres, were considered in pioneering works on the subject. With further development of sophisticated growth techniques, semiconductor systems of nanoscale dimensions became available—the well-known quantum wells, quantum well wires, quantum dots (QDs), etc.

In the present work we shall focus on QD structures, where all three spatial dimensions are strongly reduced to the nanometric scale. The important technological progress of recent years has led to processes of fabrication and thermal treatment that can produce QDs with good size distributions [2, 3]. On the other hand, using microluminescence and micro-Raman measurements, these systems can be studied at an almost individual level [4–7].

We shall be interested in polar QDs of the prototypes CdSe, CdS, CdTe, PbS, etc. They are imbedded in a host matrix which may be modelled theoretically by an infinite dielectric medium. In the late 1980s and early 1990s several works were published on the subject where QDs of this nature were used for the investigation of polar optical vibrations [8–12]. In these

works the QD is usually treated as a sphere and the vibrations are considered along the lines of the long-wavelength dielectric continuum approach. Most of them have also investigated the Fröhlich-like electron–phonon coupling Hamiltonian[3]. In addition to the usual model of QDs with spherical shape, it is important to study the effects of the deviation from this geometry on the phonon modes. In fact, there is experimental evidence, particularly from Raman scattering spectra, that several physical properties of the QD systems may be ascribed to their geometrical shape—more specifically, to the non-sphericity of the QDs [2,7,10]. For instance, the electronic energy levels and wavefunctions of spheroidal QDs have been examined [13] and observable deviations from the perfect spherical case were reported. Moreover, nowadays CdSe rod-shaped nanocrystals are synthesized with radii ranging from 1.5 to 3.3 nm and length from 4 to 20 nm [14, 15].

In the present paper we consider the polar optical vibrations of a QD with ellipsoidal geometry, in both prolate and oblate forms, within the framework of the dielectric continuum approach. We have found that deviations from the purely spherical geometries introduce significant changes in the SO phonon dispersion laws, eigenstates, and also in the electron–phonon interaction Hamiltonian, which is derived here in terms of the geometrical spheroidal parameters that characterize the QD shape. Our approach should provide an acceptable description for the SO phonons of a spheroidal QD as well as the electron–phonon interaction Hamiltonian, whenever the phonon wavelength λ_p is smaller than the QD dimensions. In the opposite case, a different treatment should be applied to the confined phonons if we look for more reliable results. For instance in [16, 17] a better description of polar optical phonons in the long-wavelength limit is achieved, by taking into account the coupled electromechanical character of the oscillations in the starting equations and in the matching boundary conditions.

The paper is organized as follows. In section 2 we give a brief summary of the applied dielectric continuum approach. Section 3 is devoted to the discussion of SO phonons for QDs with spheroidal prolate geometry and where we included a rigorous deduction of the electron–phonon Hamiltonian for the system. In section 4 the same analysis is made for the case of a QD with spheroidal oblate geometry. A discussion of the results obtained is presented in section 5.

2. General equations

For the sake of clarity, let us briefly summarize the fundamental equations of the dielectric continuum approach to the study of the optical phonon modes. They have been extensively discussed in the literature on the subject [1, 8–12]. The Born–Huang equation of motion is

$$\ddot{\boldsymbol{w}} = -\omega_T^2 \boldsymbol{w} + \sqrt{\frac{(\epsilon_0 - \epsilon_\infty)}{4\pi}\omega_T^2}\boldsymbol{E}, \tag{1}$$

where the polarization field $\boldsymbol{P}$ is given by

$$\boldsymbol{P} = \sqrt{\frac{(\epsilon_0 - \epsilon_\infty)}{4\pi}\omega_T^2}\boldsymbol{w} + \frac{\epsilon_\infty - 1}{4\pi}\boldsymbol{E}. \tag{2}$$

Here $\boldsymbol{w} = \sqrt{N\mu}\boldsymbol{u}$ and $\boldsymbol{u}$ is the relative displacement between a pair of ions of reduced mass μ in a crystal of concentration N (the reciprocal of the unit-cell volume). The other quantities are the electric field $\boldsymbol{E}$, the transverse-limit bulk frequency ω_T, and the static (high-frequency)

[3] The word 'vibron' is used by some authors in place of 'phonon' because, to a certain extent, the QD resembles a molecule. In particular, the QD 'phonon' does not involve the corresponding momentum $\hbar\boldsymbol{k}$ and is somewhat far from the standard phonon concept.

dielectric constant ϵ_0 (ϵ_∞) of the polar material. We assume the validity of the Lyddane–Sachs–Teller relation $\omega_L^2/\omega_T^2 = \epsilon_0/\epsilon_\infty$.

Considering the electric field to satisfy the quasi-static Maxwell equations, we must require that the induction field $\boldsymbol{D} = \epsilon(\omega)\boldsymbol{E} = \boldsymbol{E} + 4\pi\boldsymbol{P}$ fulfils the Gauss equation $\boldsymbol{\nabla}\cdot\boldsymbol{D} = 0$. By using the relation $\boldsymbol{E} = -\boldsymbol{\nabla}\varphi$, we arrive at the main equation in the dielectric approach:

$$\epsilon(\omega)\,\nabla^2\varphi = 0. \tag{3}$$

For all quantities in the above equations, the harmonic time dependence $f(t) \sim \exp(-\mathrm{i}\omega t)$ is implicit. Thus, the frequency-dependent dielectric function $\epsilon(\omega)$ is easily derived as

$$\epsilon(\omega) = \epsilon_\infty \frac{(\omega^2 - \omega_L^2)}{(\omega^2 - \omega_T^2)}. \tag{4}$$

The SO phonons involve electric potentials that satisfy the Laplace equation $\nabla^2\varphi = 0$. Therefore one of the possible solutions of equation (3) is $\epsilon(\omega) \neq 0$ and $\omega \neq \omega_L$. The boundary condition, associated with the continuity of the normal component of $\boldsymbol{D}$ at the interface between two different media, leads to

$$\epsilon_1\left[\frac{\partial\varphi_1}{\partial n}\right]_S = \epsilon_2\left[\frac{\partial\varphi_2}{\partial n}\right]_S. \tag{5}$$

Finally, we just add a complementary relation, which will prove rather useful later, given by

$$\boldsymbol{\nabla}\varphi = \left[\frac{\omega_T}{\epsilon_\infty - \epsilon(\omega)}\right]\sqrt{4\pi N\mu(\epsilon_0 - \epsilon_\infty)}\,\boldsymbol{u}. \tag{6}$$

3. Prolate spheroidal quantum dots

The prolate set of spheroidal coordinates ξ, η, ϕ are related to the rectangular Cartesian coordinates through the equations

$$\begin{aligned} x &= b\sqrt{(\xi^2-1)(1-\eta^2)}\cos\phi, \\ y &= b\sqrt{(\xi^2-1)(1-\eta^2)}\sin\phi, \\ z &= b\xi\eta, \end{aligned} \tag{7}$$

where $\xi \geqslant 1$, $-1 \leqslant \eta \leqslant 1$, and $0 \leqslant \phi \leqslant 2\pi$. The equation $\xi =$ constant describes an ellipsoid of revolution where the z-axis (the axis of revolution) is taken along the ellipsoid major axis, with $2b$ being its interfocal distance. Other details concerning these curvilinear coordinates can be found elsewhere (see, for instance, [18, 19]).

Let us consider the ellipsoidal surface defined by $\xi = \xi_0 =$ constant. In our model, the inner region defined by $1 \leqslant \xi \leqslant \xi_0$ is one of the polar semiconductors mentioned above, with a dielectric function $\epsilon(\omega)$, where ω is the eigenfrequency corresponding to the SO oscillation modes of the spheroidal dot. In the exterior region, defined by $\xi \geqslant \xi_0$, we shall consider the infinite medium with a dielectric constant ϵ_D independent of the frequency.

The Laplace equation is separable in this spheroidal prolate coordinate system and the solution for the model just described can be found as [18, 19]

$$\begin{aligned} \varphi^{<} &= A_{lm}R_l^m(\xi)Y_{lm}(\eta,\phi), && \xi \leqslant \xi_0, \\ \varphi^{>} &= A_{lm}(R_l^m(\xi_0)/Q_l^m(\xi_0))Q_l^m(\xi)Y_{lm}(\eta,\phi), && \xi \geqslant \xi_0. \end{aligned} \tag{8}$$

Notice that the electric potential is already continuous at $\xi = \xi_0$. The functions $R_l^m(\xi)$ and $Q_l^m(\xi)$ are defined in [19] and we shall give them here in terms of the hypergeometric function as

$$R_l^m(\xi) = \frac{(2l)!(\xi^2-1)^{m/2}\xi^{l-m}}{2^l l!(l-m)!}F\left[\frac{m-l}{2}, \frac{m-l+1}{2}, \frac{1}{2}-l, \frac{1}{\xi^2}\right], \tag{9}$$

and

$$Q_l^m(\xi) = \frac{2^m(l-m)!\Gamma(1/2)(\xi^2-1)^{m/2}}{\Gamma(l+3/2)(2\xi)^{l+m+1}} F\left[\frac{l+m+1}{2}, \frac{l+m+2}{2}, l+\frac{3}{2}, \frac{1}{\xi^2}\right]. \tag{10}$$

Here $Y_{lm}(\eta, \phi)$ are the usual harmonic spherical functions and the angular momentum quantum numbers have values $l = 1, 2, 3, \ldots$ and $|m| \leqslant l$. The functions $R_l^m(\xi)$ diverge as ξ^l when $\xi \to \infty$ but are convergent at $\xi = 1$. The functions $Q_l^m(\xi)$ converge to zero as ξ^{-l-1} when $\xi \to \infty$ and diverge logarithmically at $\xi = 1$. For $\xi_0 = 1$ the ellipsoid is deformed to one point. Thus we shall assume $\xi_0 > 1$.

The other boundary condition at $\xi = \xi_0$, given by taking $\epsilon_1 \equiv \epsilon(\omega)$ and $\epsilon_2 \equiv \epsilon_D$ in equation (5), defines the quantity

$$f_{lm}^P(\xi_0) = \frac{\epsilon(\omega)}{\epsilon_D} \equiv \left(\frac{\mathrm{d}}{\mathrm{d}\xi} \ln Q_l^m \bigg|_{\xi_0}\right)\left(\frac{\mathrm{d}}{\mathrm{d}\xi} \ln R_l^m \bigg|_{\xi_0}\right)^{-1}. \tag{11}$$

These universal parameters f_{lm}^P are independent of the nature of the constituent materials and also do not depend on the normalization of the functions R_{lm} and Q_{lm}, but do depend on the QD dimensions through ξ_0 (see the appendix). Using equation (11) we obtain, after a little algebra, the eigenfrequencies of the SO phonons in terms of these parameters as

$$\frac{\omega_{lm}^2}{\omega_T^2} = \frac{\epsilon_0 - \epsilon_D f_{lm}^P(\xi_0)}{\epsilon_\infty - \epsilon_D f_{lm}^P(\xi_0)}. \tag{12}$$

Notice that, in contrast to the purely spherical case, the eigenfrequencies depend on two indices l, m and also on the parameter ξ_0 (analogous to the sphere radius of the spherical geometry). The size dependence of SO phonon frequencies is a very peculiar feature of the spheroidal QD. It is easy to show, for $\xi_0 \to \infty$, that equation (12) reproduces the corresponding eigenfrequencies of a purely spherical QD [1, 10]:

$$\frac{\omega_l^2}{\omega_T^2} = \frac{\epsilon_0 l + \epsilon_D(l+1)}{\epsilon_\infty l + \epsilon_D(l+1)}. \tag{13}$$

In order to obtain the quantum operators associated with the phonon field let us, as a first step, introduce the quantum operator $\hat{\boldsymbol{u}}$ corresponding to the classical relative displacements of the pair of ions. We propose that

$$\hat{\boldsymbol{u}} = u_0 \boldsymbol{\nabla}[R_l^m(\xi) Y_{lm}(\eta, \phi)]\hat{a}_{lm}, \tag{14}$$

where $\hat{a}_{lm}$ is the annihilation operator for the SO phonon mode described by the suffices l, m. As usual, these operators obey bosonic commutation relations and the quantity u_0 is a constant to be determined below. Let us now recall that the classical (kinetic) energy associated with the SO vibrational field is given by $(N\mu/2)\int \dot{\boldsymbol{u}}^2 \,\mathrm{d}^3 r$, where the volume integration must be performed over the whole region inside the ellipsoid. The corresponding quantum Hamiltonian for free SO phonons will be defined by

$$\hat{H}_0 = \tfrac{1}{4} N\mu\omega_{lm}^2 \int [\hat{\boldsymbol{u}}^\dagger \cdot \hat{\boldsymbol{u}} + \hat{\boldsymbol{u}} \cdot \hat{\boldsymbol{u}}^\dagger] \,\mathrm{d}^3 r. \tag{15}$$

By writing equation (15) we have ensured the hermiticity of $\hat{H}_0$. The substitution of equation (14) into (15) leads to

$$\hat{H}_0 = \tfrac{1}{2} N\mu\omega_{lm}^2 u_0^2 \left(\int \boldsymbol{\nabla}[R_l^m Y_{lm}^*] \cdot \boldsymbol{\nabla}[R_l^m Y_{lm}] \,\mathrm{d}^3 r\right)[\hat{a}_{lm}^\dagger \hat{a}_{lm} + \tfrac{1}{2}]. \tag{16}$$

The integral in equation (16) can be rewritten in the form

$$\int_{ellipsoid} \boldsymbol{\nabla}\chi^* \cdot \boldsymbol{\nabla}\chi \, \mathrm{d}^3 r = \int_S \chi \, \boldsymbol{\nabla}\chi^* \cdot \mathrm{d}\boldsymbol{S} - \int_{ellipsoid} \chi \, \nabla^2\chi^* \, \mathrm{d}^3 r. \tag{17}$$

In equation (17) the volume integral at the rhs is zero because $\nabla^2\chi^* = 0$ (Laplace equation). The surface integral, taken over the ellipsoid's surface S with $\xi = \xi_0$, is easy to evaluate and the result is given by

$$\int_{ellipsoid} \boldsymbol{\nabla}\chi^* \cdot \boldsymbol{\nabla}\chi \, \mathrm{d}^3 r = b(\xi_0^2 - 1) R_l^m(\xi_0) \left[\frac{\mathrm{d}}{\mathrm{d}\xi} R_l^m \right]_{\xi_0} \equiv b g_{lm}(\xi_0). \tag{18}$$

Thus, the Hamiltonian of equation (16) can be rewritten as

$$\hat{H}_0 = \tfrac{1}{2} N \mu \omega_{lm}^2 u_0^2 b g_{lm}(\xi_0)(\hat{a}_{lm}^\dagger \hat{a}_{lm} + \tfrac{1}{2}). \tag{19}$$

In order to determine the constant u_0 we just require that the SO phonon Hamiltonian assumes the standard harmonic form $\hat{H}_0 = \hbar\omega_{lm}(\hat{a}_{lm}^\dagger \hat{a}_{lm} + \frac{1}{2})$. Therefore,

$$u_0^2 = \frac{2\hbar}{N\mu\omega_{lm} b g_{lm}(\xi_0)}. \tag{20}$$

From equations (14) and (20) we obtain the Hermitian operator $\hat{\boldsymbol{u}}$, after the substitution $\hat{\boldsymbol{u}} \to (\hat{\boldsymbol{u}}^\dagger + \hat{\boldsymbol{u}})/2$, as

$$\hat{\boldsymbol{u}}(\boldsymbol{r}) = \sum_{lm} \sqrt{\left[\frac{\hbar}{2N\mu\omega_{lm} b g_{lm}(\xi_0)} \right]} (\boldsymbol{\nabla}[R_l^m Y_{lm}]\hat{a}_{lm} + \mathrm{H.c.}) \tag{21}$$

where 'H.c.' stands for 'Hermitian conjugate'. The operator associated with the electric potential $\hat{\varphi}$ may be obtained from equation (6) by applying (21) and we find

$$\hat{\varphi}(\boldsymbol{r}) = \sum_{lm} \frac{\epsilon_\infty \omega_L}{\epsilon_\infty - \epsilon_D f_{lm}(\xi_0)} \left[\frac{2\pi\hbar}{\epsilon^* b \omega_{lm} g_{lm}(\xi_0)} \right]^{1/2} [R_l^m(\xi) Y_{lm}(\eta, \phi)\hat{a}_{lm} + \mathrm{H.c.}], \tag{22}$$

where $1/\epsilon^* = 1/\epsilon_\infty - 1/\epsilon_0$ and equation (12) was also used. Equation (22) represents the electric potential operator for $\xi \leqslant \xi_0$. The expression for $\hat{\varphi}(\boldsymbol{r})$ can be easily extended to the whole space in an obvious way and the result is

$$\hat{\varphi}(\boldsymbol{r}) = \sum_{lm} \frac{\epsilon_\infty \omega_L}{\epsilon_\infty - \epsilon_D f_{lm}(\xi_0)} \sqrt{\frac{2\pi\hbar}{\epsilon^* b \omega_{lm} g_{lm}(\xi_0)}} [F_l^m(\xi) Y_{lm}(\eta, \phi)\, \hat{a}_{lm} + \mathrm{H.c.}], \tag{23}$$

where

$$\begin{aligned} F_l^m(\xi) &= R_l^m(\xi), && \xi \leqslant \xi_0, \\ F_l^m(\xi) &= [R_l^m(\xi_0)/Q_l^m(\xi_0)] Q_l^m(\xi), && \xi \geqslant \xi_0. \end{aligned} \tag{24}$$

Hence, the electron–SO phonon interaction Hamiltonian is rigorously given by

$$\hat{H}_{\mathrm{e-ph}}(\boldsymbol{r}) = -e\hat{\varphi}(\boldsymbol{r}). \tag{25}$$

4. Oblate spheroidal QDs

Let us now consider ξ, η, ϕ to be oblate spheroidal coordinates which are related to orthogonal Cartesian coordinates through the equations [18, 19]

$$\begin{aligned} x &= b\sqrt{(\xi^2 + 1)(1 - \eta^2)} \cos\phi, \\ y &= b\sqrt{(\xi^2 + 1)(1 - \eta^2)} \sin\phi, \\ z &= b\xi\eta, \end{aligned} \tag{26}$$

where $\xi \geqslant 0$, $-1 \leqslant \eta \leqslant 1$, and $0 \leqslant \phi \leqslant 2\pi$. In terms of these coordinates the Laplace equation is also separable. The equations involving η and ϕ are completely coincident with the corresponding equations in the prolate spheroidal coordinate system. The equation involving ξ is somewhat different, but can be reduced to its corresponding prolate case by the transformation $\xi \to \mathrm{i}\xi$. Hence, the equation involving ξ has the same solutions as in the prolate case, but the special functions appearing there now will depend on $\mathrm{i}\xi$. However, in our treatment we shall introduce slight changes to the normalization, namely

$$R_l^m(\mathrm{i}\xi) = \frac{(2l)!}{2^l l!(l-m)!}(\xi^2+1)^{m/2}(\xi)^{l-m} F\left[\frac{m-l}{2}, \frac{m-l+1}{2}, \frac{1}{2}-l, -\frac{1}{\xi^2}\right], \tag{27}$$

since this solution becomes divergent as ξ^l when $\xi \to \infty$. For similar reasons, the other function

$$Q_l^m(\mathrm{i}\xi) = \frac{2^l l!(l+m)!}{(2l+1)!}(\xi^2+1)^{m/2}(\xi)^{-l-m-1} F\left[\frac{l+m+1}{2}, \frac{l+m+2}{2}, l+\frac{3}{2}, -\frac{1}{\xi^2}\right] \tag{28}$$

will converge to zero as ξ^{-l-1} when $\xi \to \infty$. Notice that, despite these slight differences in the normalization, we are applying the same notation as was used in the prolate case.

The equation $\xi = \xi_0 =$ constant defines the surface of an oblate ellipsoid. Now, the solutions of the Laplace equation can be written as

$$\begin{aligned} \varphi^{<}(\boldsymbol{r}) &= A_{lm} R_l^m(\mathrm{i}\xi) Y_{lm}(\eta,\phi), && \xi \leqslant \xi_0, \\ \varphi^{>}(\boldsymbol{r}) &= A_{lm} \frac{R_l^m(\mathrm{i}\xi_0)}{Q_l^m(\mathrm{i}\xi_0)} Q_l^m(\mathrm{i}\xi) Y_{lm}(\eta,\phi), && \xi \geqslant \xi_0, \end{aligned} \tag{29}$$

where the continuity of φ at $\xi = \xi_0$ is already ensured. Thus, the second boundary condition, equation (5), defines the equivalent set of universal parameters for the oblate case as

$$f_{lm}^O(\xi_0) = \frac{\epsilon(\omega)}{\epsilon_D} = \left[\frac{\mathrm{d}}{\mathrm{d}\xi} \ln Q_l^m(\mathrm{i}\xi)\bigg|_{\xi_0}\right]\left[\frac{\mathrm{d}}{\mathrm{d}\xi} \ln R_l^m(\mathrm{i}\xi)\bigg|_{\xi_0}\right]^{-1}. \tag{30}$$

An identical procedure allows the determination of the corresponding SO phonon eigenfrequencies in oblate geometry:

$$\frac{\omega_{lm}^2}{\omega_T^2} = \frac{\epsilon_0 - \epsilon_D f_{lm}^O(\xi_0)}{\epsilon_\infty - \epsilon_D f_{lm}^O(\xi_0)}, \tag{31}$$

where the modes ω_{lm} obey an equation formally analogous to equation (12), as one could guess from simple arguments, depending on the parameters $f_{lm}^O(\xi_0)$. The parameters $f_{lm}^O(\xi_0)$ have the same general properties as those discussed in the prolate case, but their dependence on ξ_0 is clearly different (see also the appendix).

In deriving the corresponding operators $\hat{\boldsymbol{u}}$ and $\hat{\varphi}$ of the SO phonons for oblate spheroids, we must follow steps analogous to those already made in the prolate case. For the sake of brevity, we just write the final results:

$$\hat{\boldsymbol{u}}(\boldsymbol{r}) = \sum_{lm}\left[\frac{\hbar}{2N\mu\omega_{lm} b \tilde{g}_{lm}(\xi_0)}\right]^{1/2} [\boldsymbol{\nabla}[R_l^m(\mathrm{i}\xi) Y_{lm}(\eta,\phi)]\hat{a}_{lm} + \mathrm{H.c.}], \tag{32}$$

and

$$\hat{\varphi}(\boldsymbol{r}) = \sum_{lm} \frac{\epsilon_\infty \omega_L}{\epsilon_\infty - \epsilon_D f_{lm}^O}\left[\frac{2\pi\hbar}{\epsilon^* \omega_{lm} b \tilde{g}_{lm}(\xi_0)}\right]^{1/2} [R_l^m(\mathrm{i}\xi) Y_{lm}(\eta,\phi)\hat{a}_{lm} + \mathrm{H.c.}], \tag{33}$$

where $\tilde{g}_{lm}(\xi_0) = (\xi_0^2 + 1)R_l^m(\mathrm{i}\xi_0)[\frac{\mathrm{d}}{\mathrm{d}\xi}R_l^m(\mathrm{i}\xi)]_{\xi_0}^*$. Equation (33) is valid just for $\xi \leqslant \xi_0$. As in the case of the prolate ellipsoid, we extend the electric potential operator to the whole space:

$$\hat{\varphi}(\boldsymbol{r}) = \sum_{lm} \frac{\epsilon_\infty \omega_L}{\epsilon_\infty - \epsilon_D f_{lm}^O} \left[\frac{2\pi\hbar}{\epsilon^* \omega_{lm} b \tilde{g}_{lm}(\xi_0)}\right]^{1/2} [\tilde{F}_l^m(\mathrm{i}\xi) Y_{lm}(\eta, \phi)\hat{a}_{lm} + \mathrm{H.c.}], \tag{34}$$

where

$$\begin{aligned} &\tilde{F}_l^m(\mathrm{i}\xi) = R_l^m(\mathrm{i}\xi), && \xi \leqslant \xi_0, \\ &\tilde{F}_l^m(\mathrm{i}\xi) = [R_l^m(\mathrm{i}\xi_0)/Q_l^m(\mathrm{i}\xi_0)]Q_l^m(\mathrm{i}\xi), && \xi \geqslant \xi_0. \end{aligned} \tag{35}$$

We have found it convenient to define the function $\tilde{F}_l^m$, instead of the function F_l^m already defined in equation (24), due to the slight differences between the normalizations of the corresponding functions R_l^m and Q_l^m. The electron–phonon Hamiltonian is again given by equation (25) with the electric potential operator taken from equation (34).

5. Discussion of the results

In order to get a deeper understanding of the theoretical results presented in the foregoing sections, let us consider the particular case of a CdSe QD imbedded in an infinite dielectric medium. The applied physical parameters are the same as in [7]: $\omega_T = 165.2\,\mathrm{cm}^{-1}$, $\epsilon_0 = 9.53$, $\epsilon_\infty = 5.72$, while for the exterior medium we take $\epsilon_D = 4.64$.

Let us analyse the dependence of the phonon frequencies ω_{lm} on the QD dimensions and geometrical shape. In figure 1(a) we present the calculated values of ω_{lm}^2, measured in units of ω_T, as a function of $1/\xi_0$ for quantum numbers $l = 1, 2$ in QDs with prolate shape. The possible SO phonon modes are explicitly indicated in the figure. The dotted lines show the corresponding values of eigenfrequencies for the strictly spherical case. It can be seen from the figure and from the appendix that the phonon frequencies follow the same trends as the corresponding parameters f_{lm}^P. The spherical modes can be asymptotically achieved in the limit $\xi_0 \to \infty$, as expected. The other limiting value $\xi_0 \to 1$ can also be attained.

In figure 1(b) we show the same calculated values of ω_{lm}^2 for a QD with oblate geometry. For QDs with oblate shape, the frequencies follow the same trends as the parameter f_{lm}^P and, therefore, display the regularity which is in contrast with the smooth dependence observed in the prolate case. The different geometry of the oblate ellipsoid leads the frequencies of the various modes to exhibit sharp contrast with those of the prolate ellipsoid. For the oblate case it was necessary to consider a wider interval of variation for the parameter $1/\xi_0$ (up to 40). Theoretically this parameter ranges up to infinity. However, the higher the value of $1/\xi_0$, the less likely the fabrication of the QD structure with dimension ξ_0. It is interesting to note that each frequency for a purely spherical QD is now split into various frequencies, according to the restriction $m \leqslant l$. Also the separation between the group of $(2m + 1)$ frequencies will depend on the QD dimensions through ξ_0. This is a very peculiar result, intrinsic to the spheroidal geometry. The frequency splittings, in general, are not very large but still can be found in a range of experimental resolution—for instance, in micro-Raman experiments. Let us remark that the frequency splittings between the different modes for an oblate ellipsoid are of the same order of magnitude as for the prolate case. However, the sign of the splitting for certain modes can be different. For example, the frequencies for the (1, 0) mode in an oblate QD are higher than the frequencies in the (1, 1) mode. It is convenient to introduce a parameter r, defined as the ratio of the ellipsoid semi-axes, and given by $r = \xi_0/\sqrt{\xi_0^2 - 1}$ ($r = \sqrt{\xi_0^2 + 1}/\xi_0$) for the prolate (oblate) ellipsoid. According to experimental observations [20] the values of the ratio are likely to be found in the range $1.1 \leqslant r \leqslant 1.3$, and it is a measure of any slight deviation

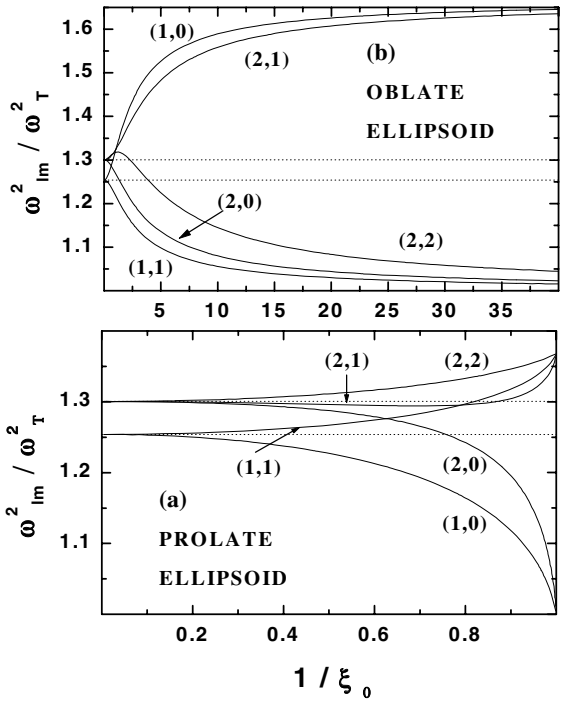

Figure 1. (a) Dependences of the squared frequencies, ω^2_{lm} in units of ω^2_T, on the QD size, $1/\xi_0$, for prolate ellipsoidal symmetry; (b) dependences of the squared frequencies, ω^2_{lm} in units of ω^2_T, for the oblate ellipsoidal symmetry. In both cases the dotted lines correspond to the strict spherical case. We use $l = 1, 2$ and all possible values of m in each case.

from sphericity. It should be noted that differences between the prolate and the oblate cases are present even for values of r very close to unity (when the QD is very near the spherical case). This peculiar behaviour is significant and indicates the sensitivity of the SO phonon frequencies to changes in the QD geometry. If we focus on the $(1, 0)$ mode, we observe that the corresponding eigenfrequency ω_{10} is lower (higher) than that for the spherical case in the prolate (oblate) case. On the other hand, the frequency ω_{21} is very near the corresponding frequency in the spherical QD for the prolate ellipsoid, but in the oblate ellipsoid it is clearly larger. We must note that such frequency differences between the prolate and the oblate cases are practically independent of the semi-axis ratio r and should be interpreted as a direct consequence of the QD topology. Let us remark that higher deviations from the spherical geometry are in principle possible, a point that will depend on the fabrication technology and requires further analysis.

In figure 2 we show the values of ω^2_{lm} (in units of ω_T) as a function of $1/\xi_0$ but taking $l = 3$. In figure 2(a) we present the prolate case while the oblate case is depicted in figure 2(b). The dotted lines, as before, represent the frequencies for the strictly spherical QD. As is explicitly shown in the figure, we are using different scales for the parameter $1/\xi_0$ corresponding to the prolate and the oblate cases. We must also remark that, for a higher value of l, the splitting magnitude decreases.

In figure 3 we depict the dependence of the eigenfrequencies ω^2_{lm} ($l = 1$ and 2) on the host material obtained by changing its dielectric constant ϵ_D for QDs with a fixed value of ξ_0 having both the prolate (figure 3(a)) and oblate (figure 3(b)) geometries. We have considered a rather

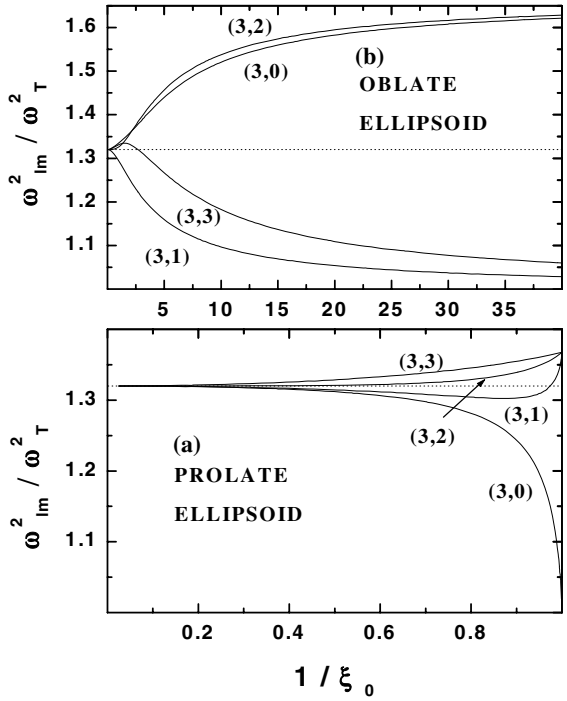

Figure 2. (a) Squared frequencies ω_{lm}^2 (in units of ω_T^2) as a function of $1/\xi_0$ for $l = 3$ and all possible values of m for the prolate ellipsoid; (b) the same, but for the oblate ellipsoid. The dotted line represents the strict spherical case.

wide range of values for ϵ_D since, as discussed in [21], if the host material is ferroelectric, this constant can reach values as large as 5000. These systems appear to have technological importance [21]. The dotted curves in the figure refer to the modes for the strictly spherical case. We have fixed $\xi_0 = 2.4$ corresponding to $r = 1.1$ in the prolate case and $r = 1.08$ in the oblate case. Notice that all curves approach asymptotically the frequency ω_T for host materials with large dielectric constant ϵ_D. This limit can also be obtained analytically from equations (12) and (31). Hence the splittings between different frequencies will decrease for host materials with large ϵ_D. Under experimental conditions, the differences between the SO phonon frequencies can be resolved just for relatively small values of ϵ_D.

In figure 4(a) we present the radial part of the electron–phonon interaction Hamiltonian $e\varphi_{lm}$, as a function of ξ, created by the SO phonons in prolate geometries. The quantity $e\varphi_{lm}$ is plotted in units of $e\varphi_0 = \sqrt{2\pi e^2\hbar\omega_L^2/\epsilon^* b\omega_T}$, for $l = 1, 2$ and for all possible m. The potential is peaked at $\xi = \xi_0$ (in the figure we fixed $\xi_0 = 2.4$), in correspondence with the interface character of the phonon modes. The slopes of the curves at the peaks are not continuous due to the different dielectric constants of the media involved. The term for $l = 3$ was not shown since the corresponding interactions are quite small (a thousand times lower) and off the scale of the figure. Hence, the modes exhibiting a stronger contribution to the electron–phonon interaction are those with the two smaller values of $l = 1, 2$. In figure 4(b) we show the same plots for the oblate QD case. From these figures we can obtain a qualitative insight into the electron–phonon interaction and its strength. Actually, the angle-dependent part of the potential is also important and can change the sign of the interaction.

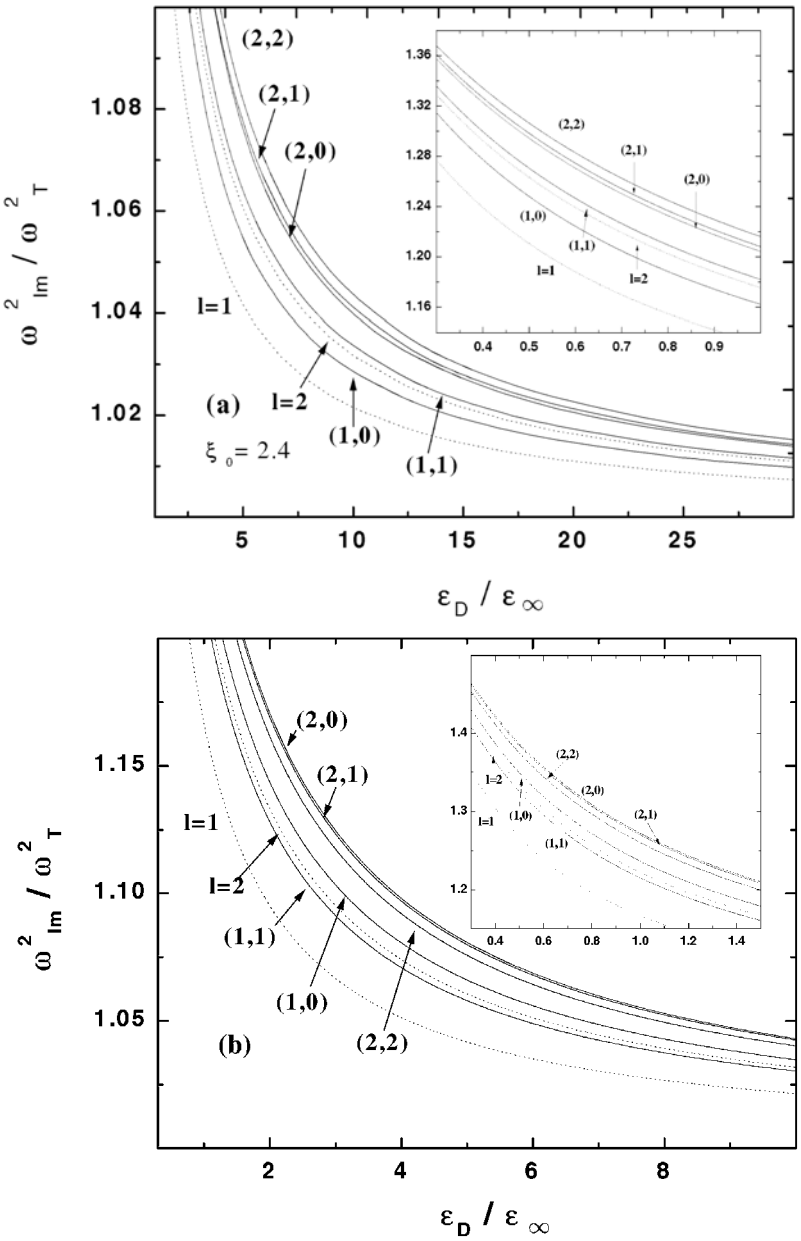

Figure 3. (a) Squared frequencies ω_{lm}^2 (in units of ω_T^2) as a function of $\epsilon_D/\epsilon_\infty$ for $l = 1, 2$ and all possible values of m for the prolate QD. In the inset the interval $0.3 \leqslant \epsilon_D/\epsilon_\infty \leqslant 1$ is shown. (b) The same, but for the oblate QD. In the inset the interval $0.3 \leqslant \epsilon_D/\epsilon_\infty \leqslant 1.5$ is shown.

A final and most interesting point concerns the selection rules for phonon-assisted first-order Raman scattering in spheroidal QD systems. SO phonons have been invoked in order to explain a certain small 'shoulder' structure experimentally observed on the lower-energy side of the main Raman peak [7, 10]. However, it has been proved that the first-order Raman selection rules forbid the corresponding transitions for purely spherical QDs [16]. On the other hand,

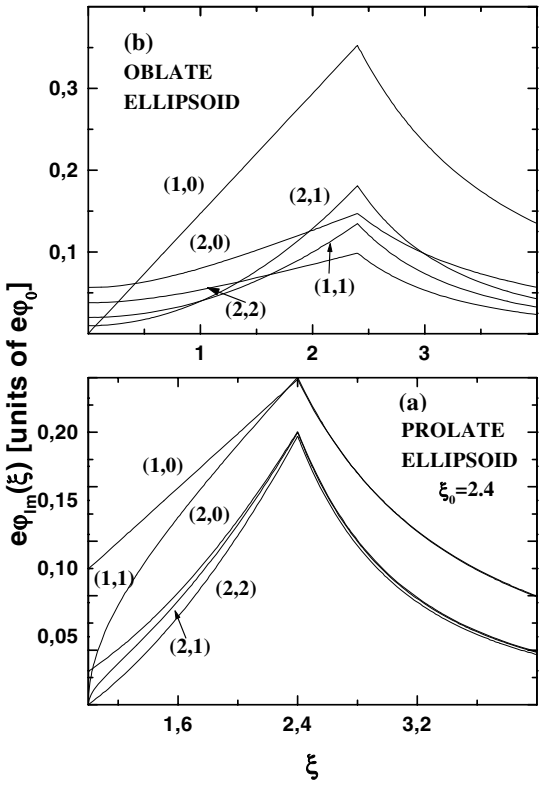

Figure 4. (a) The radial part of the electron–phonon interaction $e\varphi_{lm}$ in units of $e\varphi_0$ (see the text) as a function of ξ for $l = 1, 2$ and all possible values of m. It is clearly peaked at the QD surface (with $\xi_0 = 2.4$). (b) The same, but for the oblate QD.

in systems showing a deviation from the spherical geometry, such as the spheroidal cases discussed here, the Raman selection rules allow interface phonons with $m = 0$, $l =$ even number. Therefore, we are led to infer that a consistent explanation for the small shoulder in some line-shapes of the Raman spectra [22] can only be observed for those samples that display a certain degree $r > 1$ of deviation from the purely spherical geometry. For example, following the data taken from [7], a CdSe QD with a mean radius of 2.6 nm presents a Raman line-shape with a 'shoulder' maximum at $\approx$188 cm^{-1}. This structure can be explained by arguing that the SO phonon frequency with $l = 2$ and $m = 0$ involves a prolate QD with a ratio $r = 1.07$.

Acknowledgments

We acknowledge financial support from Fundação de Amparo à Pesquisa de São Paulo (FAPESP) and from Conselho Nacional de Desenvolvimento Científico e Tecnológico (CNPq). Also, FC and CTG are grateful to Departamento de Física, Universidade Federal de São Carlos, for hospitality. Finally, CTG thanks J Drake for helpful discussions.

Appendix

We here report the parameters f_{lm}^{P} as a function of $x = 1/\xi_0$ for several values of l, m in the case of the prolate ellipsoid:

$$f_{10}^{P} = \frac{(1-x^2)v(x) - x}{(1-x^2)v(x) - x(1-x^2)} \tag{A.1}$$

$$f_{11}^{P} = \frac{x(1-2x^2) - (1-x^2)v(x)}{x - (1-x^2)v(x)} \tag{A.2}$$

$$f_{20}^{P} = \frac{(1-x^2)v(x) + (2x^2/3 - 1)x}{(1-x^2)v(x) - 3x(1-x^2)/(3-x^2)} \tag{A.3}$$

$$f_{21}^{P} = \frac{x(6-7x^2)/(2-x^2) - 3(1-x^2)v(x)}{(3-2x^2)x - 3(1-x^2)v(x)} \tag{A.4}$$

$$f_{22}^{P} = \frac{6(1-x^2)v(x) - 2x(4x^4 - 5x^2 + 3)/(1-x^2)}{6(1-x^2)v(x) - 2x(3-5x^2)/(1-x^2)} \tag{A.5}$$

$$f_{30}^{P} = \frac{2(5-3x^2)v(x) + 2x(13x^2 - 15)(5-3x^2)/(3(1-x^2)(5-x^2))}{2(5-3x^2)v(x) - 10x + 8x^3/3} \tag{A.6}$$

$$f_{31}^{P} = \frac{5x(31-11x^2)/4 + x(25-42x^2+9x^4)/(4(1-x^2)) - 3(15-11x^2)v(x)}{10x(15-11x^2)/(5-x^2) + x(5-3x^2)(15-11x^2)/((1-x^2)(5-x^2))} \tag{A.7}$$

$$f_{32}^{P} = \frac{15(1-x^2)v(x) - (45x - 90x^3 + 49x^5)/(3 - 4x^2 + x^4)}{15(1-x^2)v(x) - (15x - 25x^3 + 8x^5)/(1-x^2)} \tag{A.8}$$

$$f_{33}^{P} = \frac{15(x^2-1)^3 v(x) + x(15 - 40x^2 + 33x^4 - 16x^6)}{15(x^2-1)^3 v(x) + x(15 - 40x^2 + 33x^4)} \tag{A.9}$$

where $v(x) = \ln[(1+x)/(1-x)]$. The corresponding parameters f_{lm}^{O} for the oblate ellipsoid are easily obtained by means of the transformation $x \to -\mathrm{i}x$ and taking into account that

$$\frac{1}{2}\ln\left(\frac{1-\mathrm{i}x}{1+\mathrm{i}x}\right) = -\mathrm{i}\tan^{-1}x.$$

References

[1] Ruppin R and Englman R 1970 *Rep. Prog. Phys.* **33** 149 and references therein
[2] Ekimov A I 1996 *J. Lumin.* **70** 1
[3] Bertram D 1998 *Phys. Rev.* B **57** 4265
[4] Pusep Yu A, Zanelatto G, da Silva G S, Galzerani J C, Gonzalez-Borrero P P, Toropov A I and Basmaji P 1998 *Phys. Rev.* B **58** R1770
[5] Empedocles S A, Norris D J and Bawendi M G 1996 *Phys. Rev. Lett.* **77** 3877
[6] Norris D J, Sacra A, Murray C B and Bawendi M G 1994 *Phys. Rev. Lett.* **72** 2612
[7] Trallero-Giner C, Debernardi A, Cardona M, Menendez-Proupin E and Ekimov A I 1998 *Phys. Rev.* B **57** 4664
[8] Schmitt-Rink S, Miller D A B and Chemla D S 1987 *Phys. Rev.* B **35** 8113
[9] Alivisatos A P, Harris T D, Carrol P J, Steigerwald M L and Brus L E 1989 *J. Chem. Phys.* **90** 3463
[10] Klein M C, Hache H, Ricard D and Flytzanis C 1990 *Phys. Rev.* B **42** 11 123
[11] Nomura S and Kobayashi T 1992 *Phys. Rev.* B **45** 1305

[12] Bawendi M G, Carrol P J, Wilson W L and Brus L E 1992 *J. Chem. Phys.* **96** 946
[13] Cantele G, Ninno D and Iadonisi G 2000 *J. Phys.: Condens. Matter* **12** 9019 and references therein
[14] Peng X, Manna L, Yang W, Wickham J, Scher E, Kadavanich A and Alivisatos A P 2000 *Nature* **404** 59
[15] Li L, Hu J, Yang W and Alivisatos A P 2001 *Nano Lett.* **1** 349
[16] Roca E, Trallero-Giner C and Cardona M 1994 *Phys. Rev.* B **49** 13 704
[17] Chamberlain M P, Trallero-Giner C and Cardona M 1995 *Phys. Rev.* B **51** 1680
[18] Morse P M and Feshbach H 1953 *Methods of Theoretical Physics* (New York: McGraw-Hill)
[19] Abramowitz M and Stegun I (ed) 1972 *Handbook of Mathematical Functions* (New York: Dover) p 751
[20] Nirmal N, Norris D J, Kuno M, Bawendi M G, Efros Al L and Rosen M 1995 *Phys. Rev. Lett.* **75** 3728
[21] Zhou J, Li L, Gui Z, Buddhudu S and Zhou Y 2000 *Appl. Phys. Lett.* **76** 1540
[22] Comas F, Trallero-Giner C, Studart N and Marques G E 2002 *Phys. Rev.* B **65** 073303